

Supporting Information

Growth and auto-oxidation of Pd on single-layer AgO_x/Ag(111)

Vikram Mehar¹, Christopher R. O'Connor², Tobias Egle^{2,3}, Mustafa Karatok², Robert J. Madix³,
Cynthia M. Friend^{2,3} and Jason F. Weaver^{1*}

¹Department of Chemical Engineering, University of Florida, Gainesville, FL 32611, USA

²Department of Chemistry and Chemical Biology, Harvard University, Cambridge, MA 02138, USA

³School of Engineering and Applied Sciences, Harvard University, Cambridge, MA 02138, USA

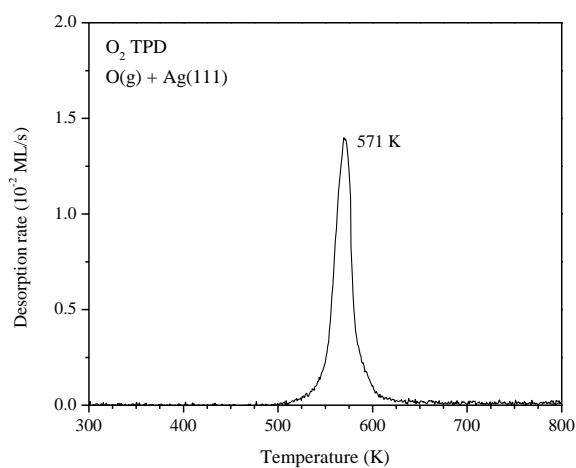
*To whom correspondence should be addressed, weaver@che.ufl.edu

Tel. 352-392-0869, Fax. 352-392-9513

S1. O₂ TPD and LEED after Ag(111) oxidation with ozone vs. atomic oxygen

Nominally the same single-layer AgO_x structure can be prepared on Ag(111) by oxidizing with atomic oxygen or ozone at 500 K, followed by flashing to 520 K in UHV. Similar LEED patterns are observed after generating the single-layer AgO_x/Ag(111) surface using atomic oxygen or ozone and the corresponding O₂ TPD spectra each exhibit a single peak and shape (Figure S1a, b). The O₂ peak temperatures are observed at 571 K vs. 578 K in experiments performed using atomic oxygen vs. ozone, respectively, due to differences in thermocouple calibrations as well as heating rates employed at University of Florida and Harvard.

a) Atomic oxygen



b) Ozone

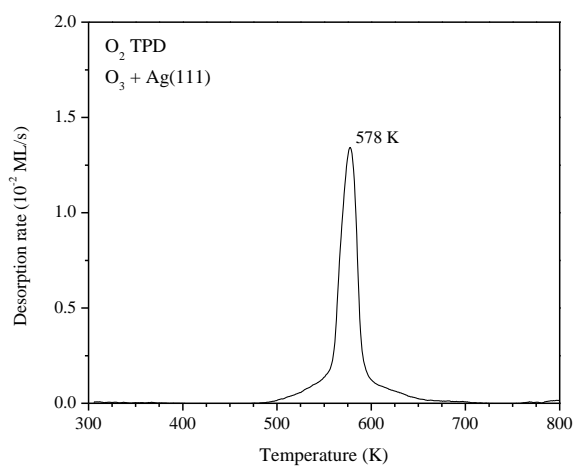
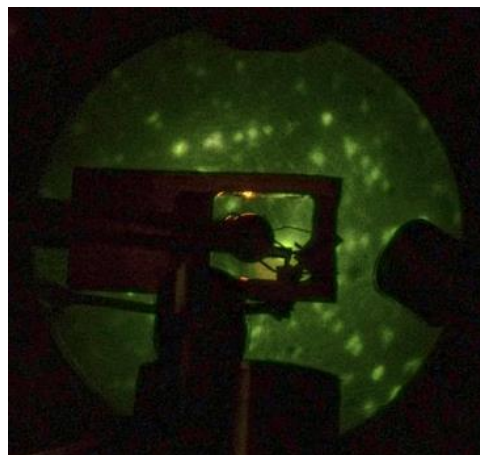


Figure S1: LEED and O₂ TPD obtained after preparing a single-layer AgO_x phase on Ag(111) using a) atomic oxygen and b) ozone. The Ag(111) sample was exposed to the oxidant at 500 K to generate an oxygen coverage of 0.38 ML, and then flashed to 520 K to improve ordering. The O₂ TPD spectra obtained after oxidizing with atomic oxygen vs. ozone were obtained using heating rates of 1 K/s vs. 3 K/s, respectively. The higher heating rate is also partly responsible for the higher O₂ peak temperature observed in the experiments with ozone.

S2. LEED from single-layer AgO_x/Ag(111) at 500 K vs. flashing to 520 K

Figure S2a shows the LEED pattern obtained after oxidizing the Ag(111) crystal with atomic oxygen at 500 K. The spot positions agree well with those simulated for the $c(3 \times 5\sqrt{3})$ single-layer oxide phase (Figure S2b). LEED also shows that heating to 520 K in UHV induces a change in the oxide surface structure. The LEED pattern shown in Fig S2c exhibits spots consistent with the $p(4 \times 5\sqrt{3})$ oxide (Figure S2d) while characteristics of the $c(3 \times 5\sqrt{3})$ structure are less evident. The dark region in the upper right of the LEED patterns is caused by charging of the sample holder. All of the results reported in this study were obtained using single-layer AgO_x/Ag(111) surfaces that yield the LEED pattern shown in Figure S2c, for which the $p(4 \times 5\sqrt{3})$ structure is dominant.

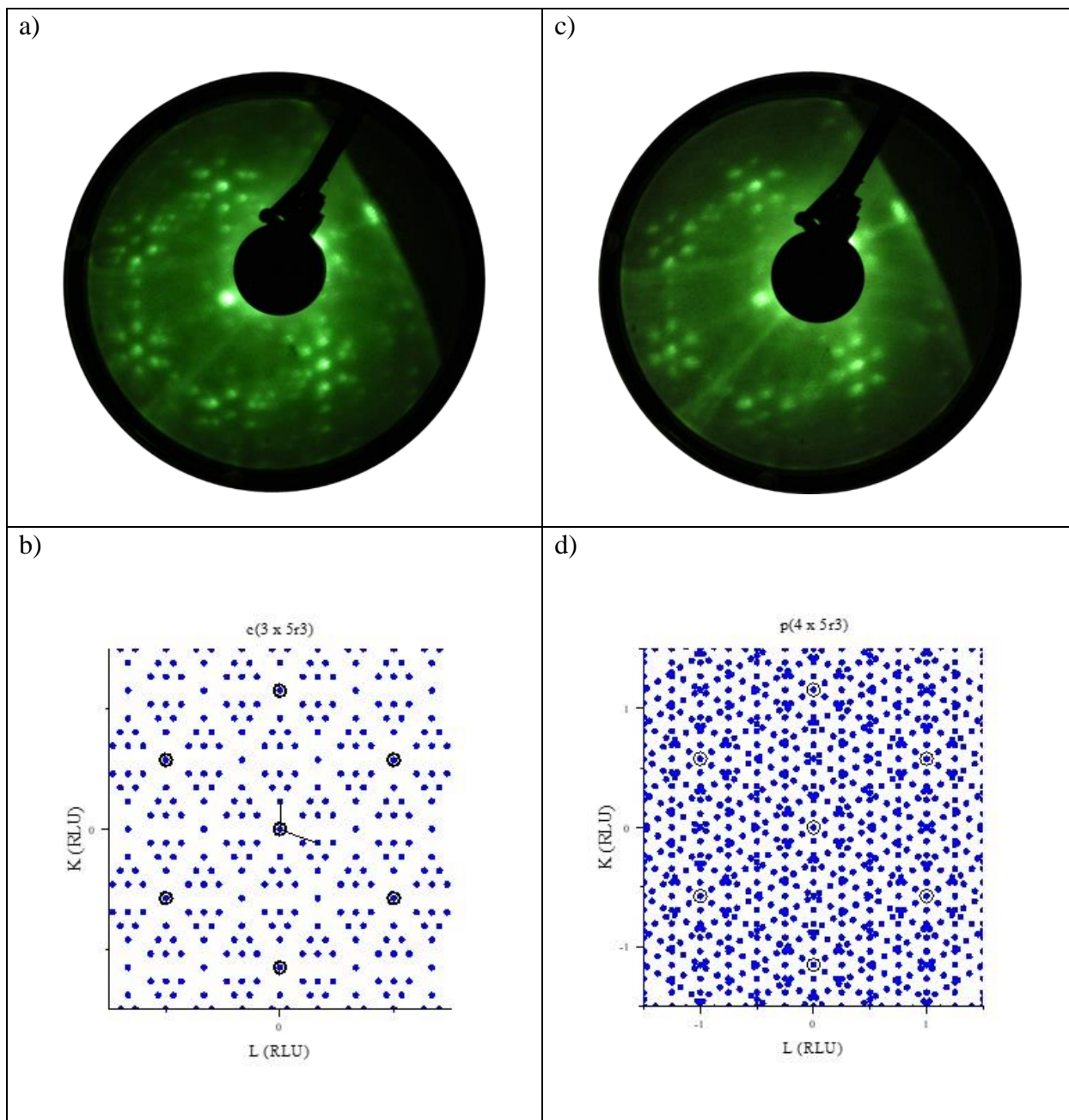
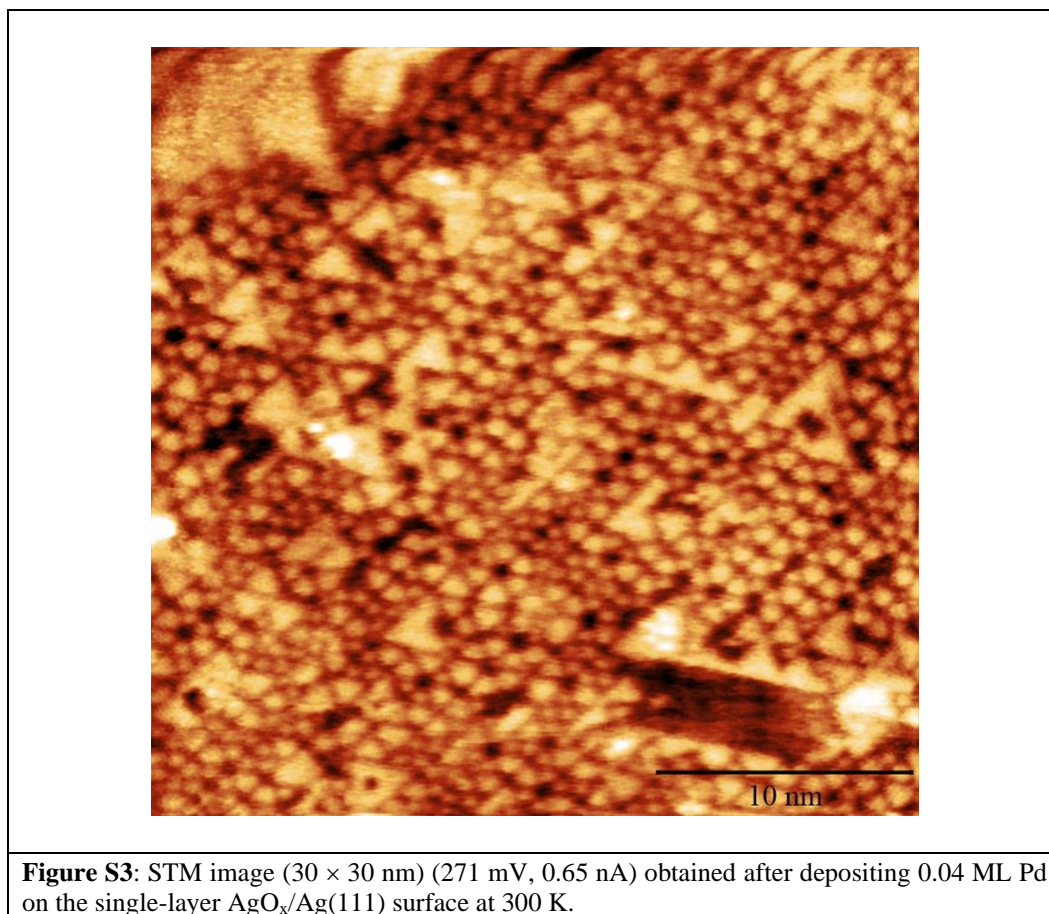


Figure S2: a) Measured and b) simulated LEED patterns (118 eV) of $c(3 \times 5\sqrt{3})$ AgO_x on Ag(111). c) Measured and d) simulated LEED patterns (118 eV) of $p(4 \times 5\sqrt{3})$ AgO_x on Ag(111) obtained after generating ~ 0.38 ML of oxygen on pristine Ag(111) at 500 K using an O-atom beam a) and after heating to 520 K in UHV c). LEED patterns were simulated for multiple rotational domains using the unit cells reported by Schnadt et al.¹

S3. High resolution image from 0.04 ML Pd-AgO_x/Ag(111)

Figure S3 shows an atomically-resolved STM image obtained after depositing 0.04 ML Pd on a single-layer AgO_x/Ag(111) surface. Triangular Pd structures with an apparent height of 0.08 nm and an average diameter of 1.0 nm are evident in the image.



S4. Analysis of STM images

The scanning tunneling microscopy measurements were analyzed using Scanning Probe Image Processor Software by Image Metrology. The STM images were levelled by adjusting the x-tilt and y-tilt to ensure the terraces were uniformly flat for particle and pore detection analysis. The particle statistics were calculated by using the particle and pore detection independently on each Ag oxide terrace with the same threshold height detection for all coverages examined. For all coverages investigated, statistics were calculated on features with an apparent height of 0.08 nm, 0.14 nm and 0.25 nm. The particle and pore detection function was not able to differentiate AgO_x and Pd particles for the 0.08 nm apparent height features for [Pd] ≤ 0.15 ML because of the similar height corrugation of Pd and AgO_x. Therefore, the 0.08 nm apparent height features containing Pd (f_I) were determined by calculating the difference between all features (f_I^{total}) and the features detected on pure AgO_x ($f = 22.6\%$). The 0.08 nm apparent height features containing Pd were not able to be reliably determined for [Pd] ≥ 0.15 ML because the disordering in the AgO_x layer caused the particle identification statistics to vary significantly with small changes in the detection height. Therefore, we assume that the fractional coverage of 0.08 nm apparent height features for [Pd] ≥ 0.15 ML to be zero. This assumption appears reasonable because we observe a linear correlation between Pd coverage as determined by quantitative analysis for the Pd coverage using AES and the Pd coverage using our layer model for fractional area (Figure 4B).

Table S1. Structural properties of Pd domains as a function of the total Pd coverage (ML) determined from statistical analysis of STM images. Structural properties listed in the table include the fractional area of the surface and average diameter of Pd domains for features with apparent heights of 0.08, 0.14 and 0.25 nm.

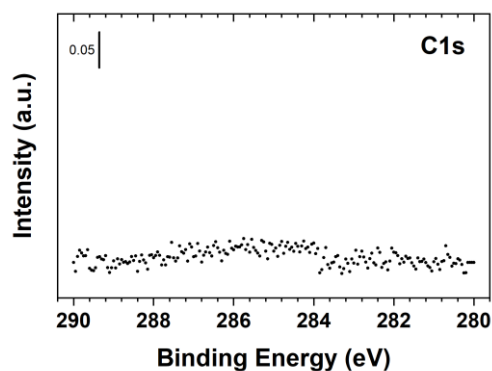
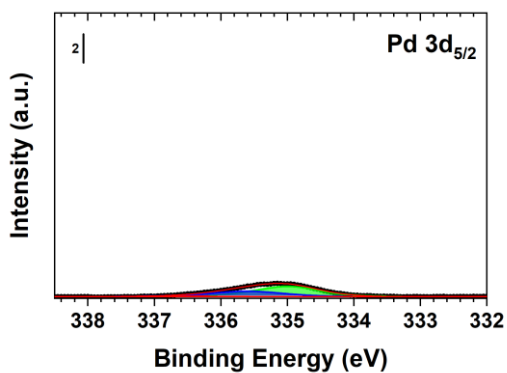
Pd coverage (ML)	0.08 nm apparent height			0.14 nm apparent height		0.25 nm apparent height	
	Fractional total area (f_i^{total})	Fractional Pd area (f_i)	Average diameter (nm)	Fractional Pd area (f_2)	Average diameter (nm)	Fractional Pd area (f_3)	Average diameter (nm)
0	22.6	0	0.7	0	-	0	-
0.04	29.3	6.7	1.0	0.2	0.7	0	-
0.08	33.4	10.8	1.4	0.3	0.9	0	-
0.15	40.5	17.9	1.4	1.5	0.8	0	-
0.30	-	0 ^a	-	17.6	2.7	0	-
0.45	-	0 ^a	-	20.7	2.8	0	-
0.90	-	0 ^a	-	48.6	6.5	0.8	1.9
1.8	-	0 ^a	-	84.8	36.1	9.7	3.5

^a Value assumed to be zero because 0.08 nm apparent height Pd clusters were neglected for [Pd] \geq 0.30 ML

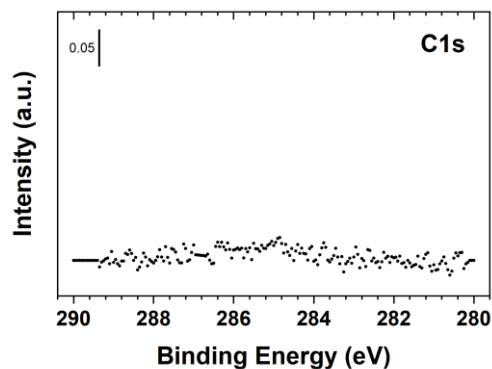
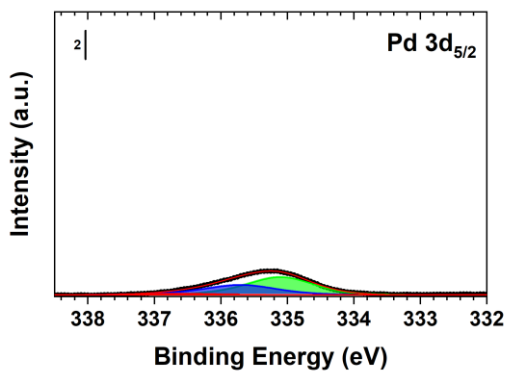
S5. XPS spectra from Pd-AgO_x/Ag(111) surfaces

The spectra acquired on Ag(111) and Pd/Ag(111) were fitted using a Doniach-Šunjić function² convoluted with a Gaussian function and background lines obtained from Shirley's method.³ The Pd core-level shifts (CLS) of CO and Pd oxide were determined in previous measurements. Pd was extensively oxidized to acquire the exact binding energy of the Pd oxide CLS. The Pd-CO CLS was determined by exposure of CO to clean Pd(111).

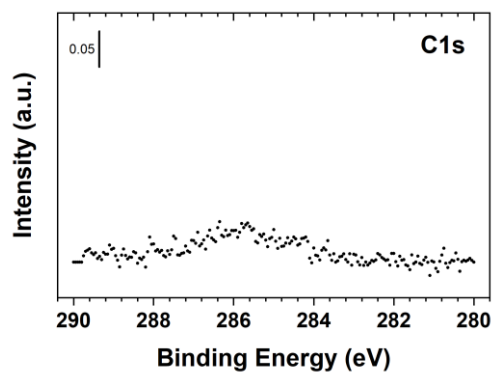
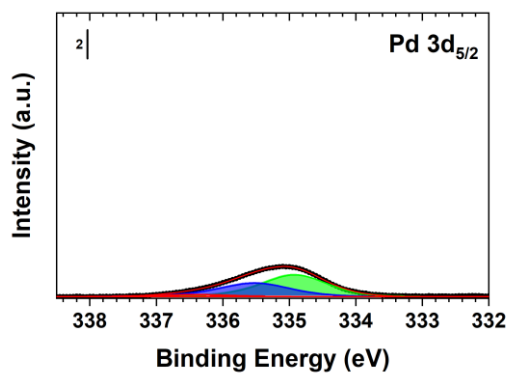
a)



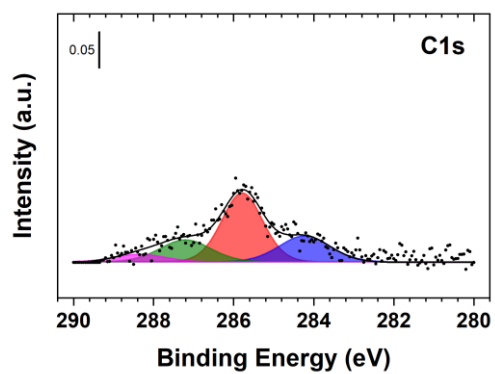
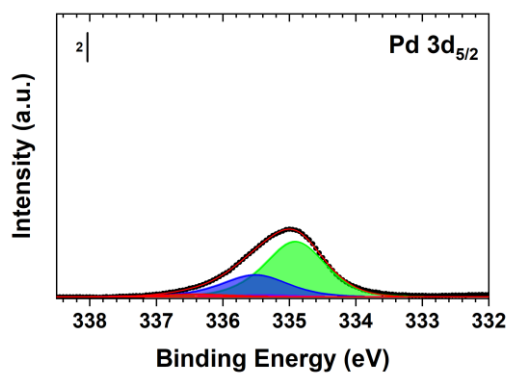
b)



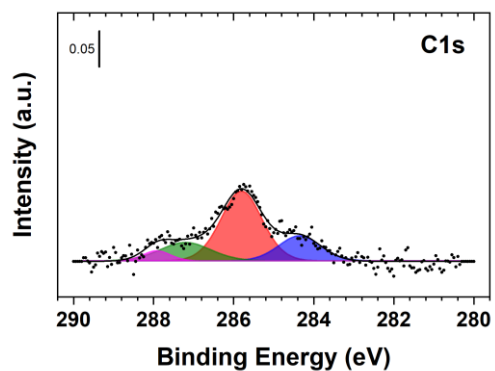
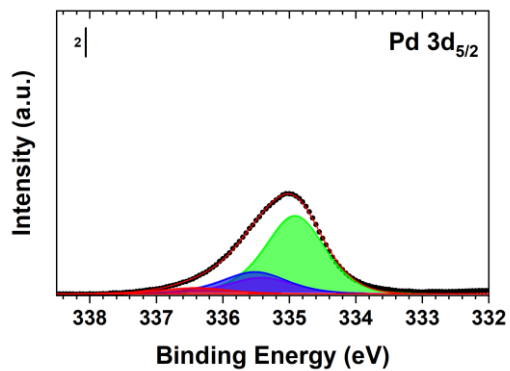
c)



d)



e)



f)

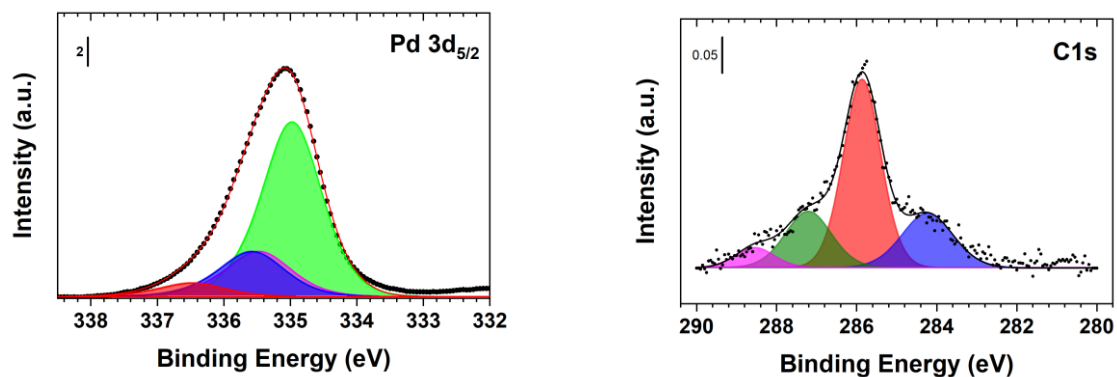
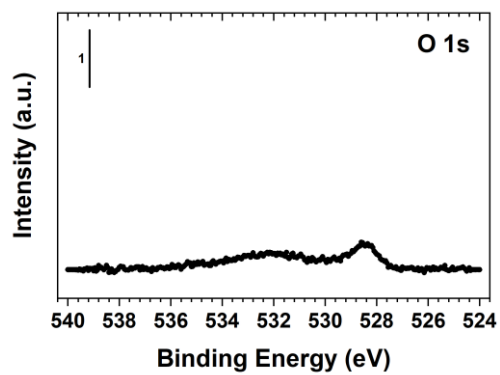
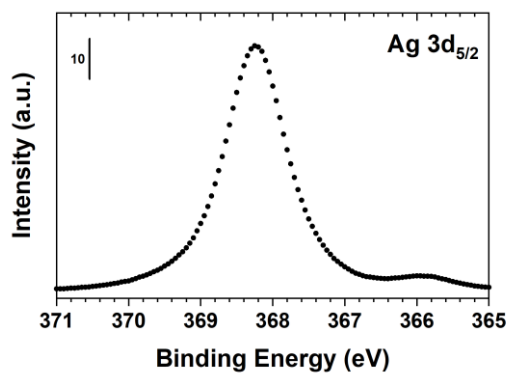
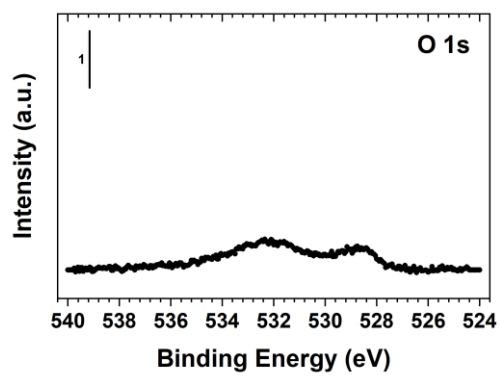
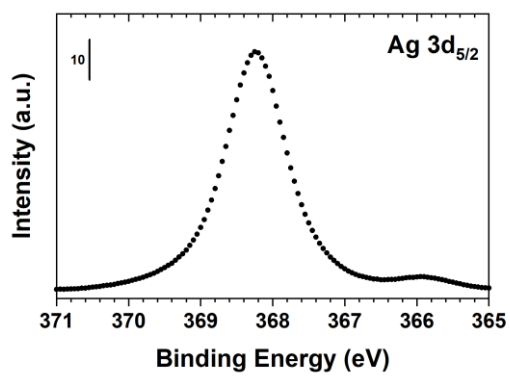


Figure S4: Pd 3d_{5/2} and C 1s XPS spectra from Pd-AgO_x/Ag(111) surfaces at Pd coverages of (a) 0.15 ML, (b) 0.25 ML, (c) 0.31 ML, (d) 0.66 ML, (e) 0.99 ML, (f) 2.5 ML. Peak assignments in Pd 3d_{5/2} spectral region (left): (light green) 335.0 eV metallic Pd, (blue) 335.5 eV Pd coordinated to two O atoms, (pink) 335.4 eV CO/Pd, (red) 336.4 eV Pd coordinated to four O atoms. Peak assignments in the C 1s spectral region (right): (blue) 284.4 eV adventitious carbon, (red) 285.8 eV CO/Pd, (green) 287.5 eV Ag₂CO₃/AgHCO₃, (purple) 287.9 eV CO/Pd oxide.

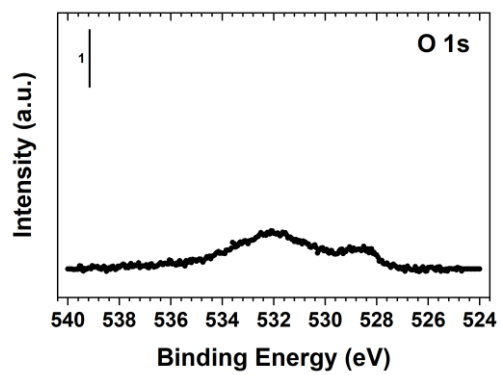
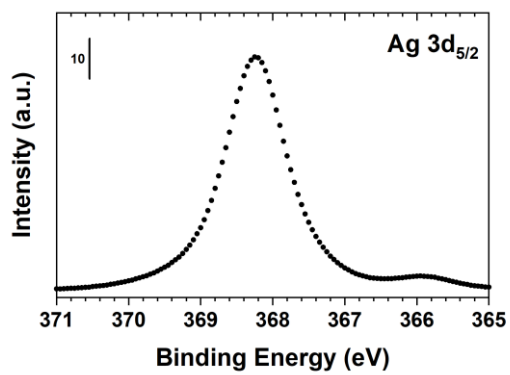
a)



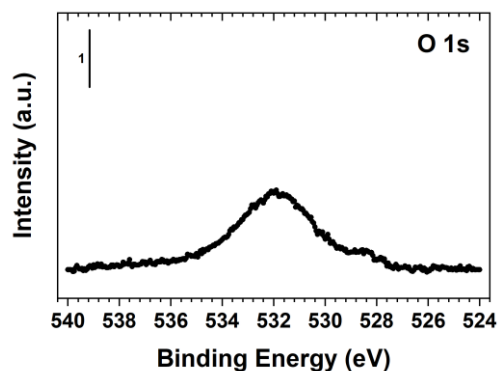
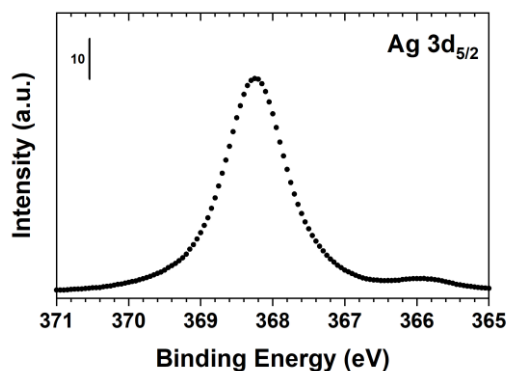
b)



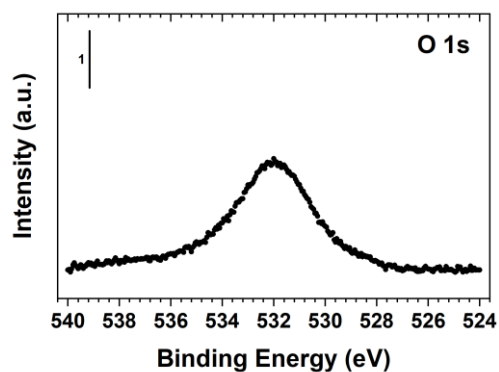
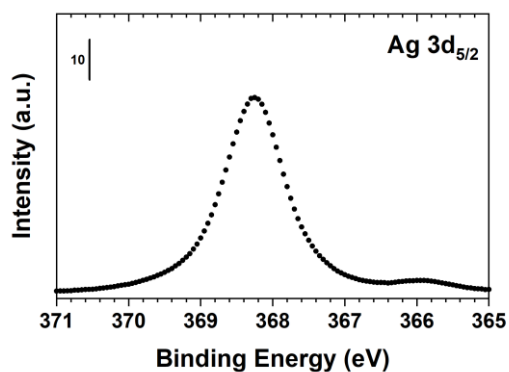
c)



d)



e)



f)

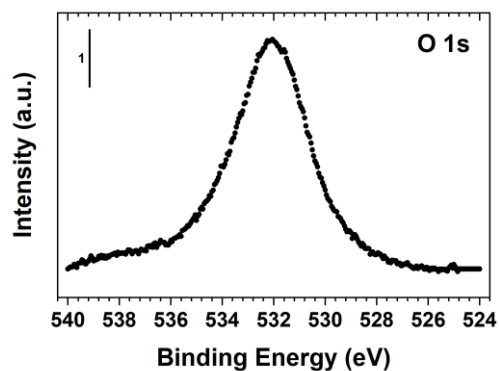
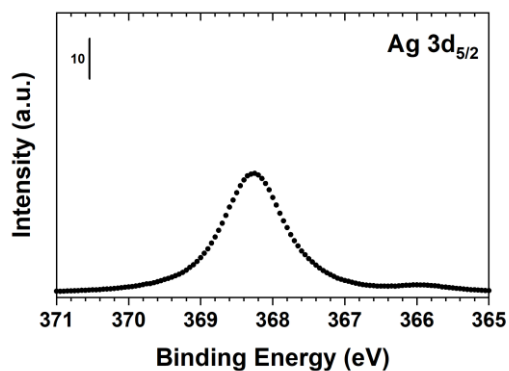


Figure S5: Ag $3d_{5/2}$ and O $1s$ XPS spectra from Pd-AgO_x/Ag(111) surfaces at Pd coverages of (a) 0.15 ML, (b) 0.25 ML, (c) 0.31 ML, (d) 0.66 ML, (e) 0.99 ML, (f) 2.5 ML. The Ag $3d_{5/2}$ and O $1s$ spectral regions are shown to the left and right, respectively. There are two prominent contributions of metallic Pd (532 eV) and ordered AgO_x (528.3 eV) in the O $1s$ spectra. Further, we expect an additional six (6), less prominent contributions in the O $1s$ spectral region: disordered oxygen in AgO_x, oxygen coordinated to four Pd atoms, oxygen coordinated to three Pd atoms, CO/ Pd oxide, CO/ Pd, Ag₂CO₃/AgHCO₃.

Table S2. Integrated relative areas of peaks in Pd3d_{5/2} spectral region as a function of Pd coverage.

Pd coverage in ML	Pd	Pd-2O	Pd-4O	CO/Pd	Total Pd-O
0.15	61.7%	35.6%	2.7%	0.0%	38.3%
0.25	59.5%	36.4%	4.1%	0.0%	40.5%
0.31	56.1%	38.5%	5.4%	0.0%	43.9%
0.66	65.9%	28.8%	3.3%	2.1%	32.1%
0.99	61.8%	19.0%	5.1%	14.1%	24.1%
2.5	60.5%	17.2%	5.2%	17.2%	22.3%

1. Schnadt, J.; Knudsen, J.; Hu, X. L.; Michaelides, A.; Vang, R. T.; Reuter, K.; Li, Z. S.; Laegsgaard, E.; Scheffler, M.; Besenbacher, F., Experimental and theoretical study of oxygen adsorption structures on Ag(111). *Phys. Rev. B* **2009**, *80*.
2. Doniach, S.; Sunjic, M., Many-Electron Singularity in X-Ray Photoemission and X-Ray Line Spectra from Metals. *Journal of Physics Part C Solid State Physics* **1970**, *3*, 285.
3. Shirley, D. A., High-Resolution X-Ray Photoemission Spectrum of Valence Bands of Gold. *Phys. Rev. B* **1972**, *5*, 4709.